Seasonal predictions of ice extent in the Arctic Ocean

R. W. Lindsay,[1] J. Zhang,[1] A. J. Schweiger,[1] and M. A. Steele[1]

Received 10 April 2007; revised 14 September 2007; accepted 9 November 2007; published 29 February 2008.

[1] How well can the extent of arctic sea ice be predicted for lead periods of up to one year? The forecast ability of a linear empirical model is explored. It uses as predictors historical information about the ocean and ice obtained from an ice–ocean model retrospective analysis. The monthly model fields are represented by a correlation-weighted average based on the predicted ice extent. The forecast skill of the procedure is found by fitting the model over subsets of the available data and then making subsequent projections using independent predictor data. The forecast skill, relative to climatology, for predictions of the observed September ice extent for the pan-arctic region is 0.77 for six months lead (from March) and 0.75 for 11 months lead (from October). The ice concentration is the most important variable for the first two months and the ocean temperature of the model layer with a depth of 200 to 270 m is most important for longer lead times. The trend accounts for 76% of the variance of the pan-arctic ice extent, so most of the forecast skill is realized by determining model variables that best represent this trend. For detrended data there is no skill for lead times of 3 months or more. The forecast skill relative to the estimate from the previous year is lower than the climate-relative skill but it is still greater than 0.45 for most lead times. Six-month predictions are also made for each month of the year and regional three-month predictions are made for 45-degree sectors. The ice-ocean model output significantly improves the predictive skill of the forecast model.

Citation: Lindsay, R. W., J. Zhang, A. J. Schweiger, and M. A. Steele (2008), Seasonal predictions of ice extent in the Arctic Ocean, *J. Geophys. Res.*, *113*, C02023, doi:10.1029/2007JC004259.

1. Introduction

[2] Sea ice is the focus of much research regarding long-term changes in response to changing greenhouse gas forcings. Seasonal forecasts of the ice conditions could play an important role in planning activities by shipping interests and coastal communities throughout the Arctic. In particular, knowing if and when shipping lanes might be ice free, when fishing grounds might clear, or the likely extent of nearshore open water that could contribute to beach erosion are all useful pieces of information. The North American Ice Service (a collaboration of the Canadian Ice Service and the U. S. National Ice Center) produces summer outlooks of ice conditions for specific regions, typically in the late spring, but does not focus on the Arctic as a whole or examine other seasons of the year. There have been some recent efforts made to develop statistical forecasts of arctic sea ice extent at seasonal to annual time periods either for the basin as a whole or for specific regions.

[3] Early efforts were made by *Barnett* [1980] and *Walsh* [1980] to predict the ice extent in the Bering, Chukchi, and Beaufort seas. Barnett used the strength of the Siberian High in April to forecast the ice severity near Barrow in August with indeterminate results. His studies led to the definition of the Barnett Severity Index (BSI) to measure the navigability of the summer waters north of Alaska. Walsh used empirical orthogonal functions of the sea level pressure, the surface air temperature, and the ice extent as predictors of the ice extent for all months of the year along the Alaskan coast. He found significant skill at lead times of 1 to 2 months and concluded this was the limit of forecasting ability using those predictors.

[4] *Drobot and Maslanik* [2002] constructed a linear regression model to forecast the end-of-summer ice conditions in the Beaufort Sea as represented in the BSI a few months in advance. It is based on four predictors: winter multiyear ice concentration, spring (May and June) total ice concentration, March North Atlantic Oscillation index, and October East Atlantic index. The model explains about 90% of the variance in the BSI for 1979–2000 within a lead time of two months.

[5] *Johnson et al.* [1985] investigated stationary and cyclostationary (seasonally dependent) forecast models for the detrended seasonal ice extent in 30° longitudinal sectors, using data from 1953–1977. They used as predictors the ice extent in each sector (persistence) and in its east and west neighbors, the air pressure gradient near the sector, the air temperature (1000–700 mb thickness), and the sea surface temperature averaged over large regions of the North Atlantic or North Pacific oceans. The hindcast skill varied greatly with the sector and the season. The best seasonal

[1]Polar Science Center, Applied Physics Laboratory, University of Washington, Seattle, Washington, USA.

0148-0227/08/2007JC004259$09.00

predictions were for the summer or winter months. None of their models, however, had any skill at lead times over 6 months, and most sectors had skill at a lead time of only two months.

[6] *Rigor et al.* [2002] studied the response of sea ice to the Arctic Oscillation (AO) index. They found that the summertime sea ice concentration (SIC) is strongly correlated with the AO index of the previous winter. A high winter AO induces changes in sea ice motion that advect more ice out of the East Siberian and Laptev seas, resulting in thinner ice there, and a consequent increase in heat flux from the ocean to the atmosphere that is responsible for warmer surface air temperatures (SAT). They state, "The correlations between the wintertime AO and SIC and SAT during the subsequent seasons offers the hope of some predictability."

[7] A Markov model for predicting the ice concentration in Antarctica was developed by *Chen and Yuan* [2004]. They used a multivariate EOF approach to reduce the number of variables and obtained good skill for the forecast of the ice concentration in some locations for up to one year in advance.

[8] *Drobot et al.* [2006] developed a statistical model to predict the pan-arctic minimum ice extent based on multiple linear regression and used the satellite-observed ice concentration, the surface skin temperature, the albedo, and the downwelling longwave radiative flux as predictor variables. Their analysis includes prediction periods of up to seven months (February to September). In all cases the ice concentration was the most important predictor, but in some months the skin temperature or the downwelling radiative flux also contributed to the model. The fraction of the interannual variance of the minimum ice extent (R^2) for their fit of the minimum ice extent went from 0.90 in August to 0.46 in February. The predictive skill was not determined for years beyond those used in the fitting of the model. This work was extended to regional predictions of the ice extent using similar predictive variables [*Drobot*, 2007]. The predictions were for the minimum September ice extent using either June or March data and were made for each of four different regions.

[9] Here an important additional source of information about the ice and ocean system is utilized to formulate predictor variables. A retrospective analyses of the coupled ice-ocean system is used to determine not only the observed ice extent and concentration, but the model mean ice thickness, the ice thickness distribution, and ocean temperature, salinity, and currents, which can all be used as potential predictors. Can this additional information be used to increase the skill of an empirical forecast model over one that uses surface data only? If so, what variables of the system are most helpful and why? Does the integrated effect of previous months or years of daily forcing (temperatures, winds, and clouds) create conditions within the ice–ocean system that are predictive of the future ice extent? What is the role of the trends in forming predictions? And finally, how predictable is sea ice extent with empirical models?

[10] The primary focus here is on the pan-arctic September mean ice extent but the monthly mean extent in other months and in regional sectors are considered as well. The ice-ocean model and the statistical methods will be introduced in section 2; the results for the entire basin will be shown in section 3 along with an analysis of the forecast model and its skill; results for other months of the year and for the different regional sectors are in section 4; a discussion follows in section 5. The predictive schemes presented here may point the way for planners to evaluate the likely future ice extent in individual sectors of the Arctic Ocean as well as understand the uncertainty of the forecasts.

2. Methods

2.1. Ice-Ocean Numerical Model

[11] We use a coupled ice–ocean model that has been applied in a wide range of retrospective climate studies [e.g., *Zhang and Rothrock*, 2005; *Lindsay and Zhang*, 2005]. The model is a Pan-arctic Ice-Ocean Modeling and Assimilation System (PIOMAS) based on the Parallel Ocean and Ice Model (POIM) of *Zhang and Rothrock* [2003]. It consists of the Parallel Ocean Program (POP) ocean model developed at Los Alamos National Laboratory coupled to a multicategory thickness and enthalpy distribution (TED) sea ice model [*Zhang and Rothrock*, 2001; *Hibler*, 1980]. The POP model is a Bryan–Cox–Semtner type ocean model [*Bryan*, 1969; *Cox*, 1984; *Semtner*, 1976] with numerous improvements, including an implicit free-surface formulation of the barotropic mode and model adaptation to parallel computing [e.g., *Smith et al.*, 1992; *Dukowicz and Smith*, 1994]. The ice model is a multicategory ice thickness and enthalpy distribution model that consists of five main components: 1) a momentum equation that determines ice motion, 2) a viscous-plastic ice rheology that determines the internal ice stress, 3) a heat equation that determines ice temperature profile and ice growth or decay, 4) an ice thickness distribution equation that conserves ice mass, and 5) an enthalpy distribution equation that conserves ice thermal energy. The TED sea ice model has eight categories each for ice thickness, ice enthalpy, and snow depth; it uses an efficient ice dynamics model [*Zhang and Hibler*, 1997] to solve the ice momentum equation with a teardrop plastic ice rheology that allows biaxial tensile stress [*Zhang and Rothrock*, 2005]. The maximum ice thickness in each bin is 0.10 m (the open water class), 0.66, 1.93, 4.20, 7.74, 12.74, 19.31, and 27.51 m.

[12] The PIOMAS configuration is based on a generalized orthogonal curvilinear coordinate system, covering the Arctic Ocean, North Pacific, and North Atlantic. The northern grid pole is displaced into Greenland and the mean horizontal resolution is about 22 km for the Arctic Ocean, Barents and GIN (Greenland-Iceland-Norwegian) seas, and Baffin Bay. The ocean model's vertical dimension has 25 levels of varying thicknesses (the first eleven levels are centered at 5.0, 15.0, 25.0, 35.0, 45.0, 55.7, 70.7, 93.7, 126.8, 172.6, and 234.1 m). The bathymetry data set is obtained by merging the IBCAO (International Bathymetric Chart of the Arctic Ocean) data set and the ETOPO5 (Earth Topography Five Minute Gridded Elevation Data Set) data set [see *Holland*, 2000]. The POP ocean model is modified so that open boundary conditions can be specified on the model's southern boundaries along 43°N. The open boundary conditions are obtained from a global POIM [*Zhang*, 2005]. They include monthly sea surface height and ocean velocity, temperature, and salinity at all depths over the period 1958–2005.

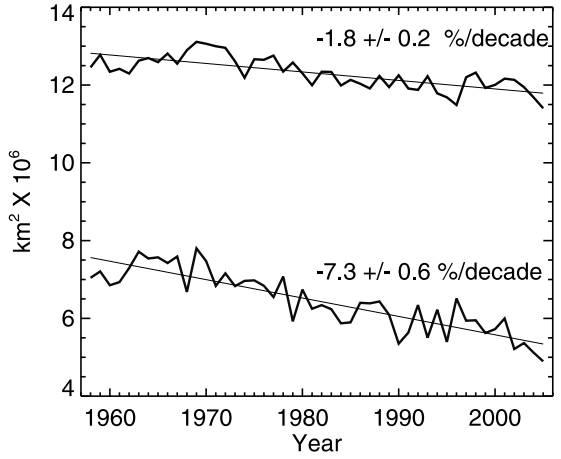

Figure 1. Time series of observed March (upper) and September (lower) ice extent from the HadSST data set with linear trend lines for the 48-year period 1958–2005.

2.1.1. Forcing Data

[13] The model is forced with daily fields of 10-m surface wind velocities, 2-m air temperature and humidity, precipitation, and downwelling long- and short-wave radiative fluxes, which are obtained from the ERA-40 Reanalysis for the period 1958–2001 and from the ECMWF operational analysis from 2002 to 2005, forty-eight years in all. We have used the ERA-40 data instead of those from NCEP because the downwelling radiative fluxes are much closer in the ERA-40 data to observations made at SHEBA and in other field programs [*Schweiger*, 2004; *Liu et al.*, 2005].

2.1.2. Ice Concentration Data

[14] The ice concentration data used to build the forecast model and used for validation is from the Hadley monthly mean observed ice concentration and SST fields, HadSST1.1, obtained from the British Atmospheric Data Centre. This data set, on a 1-degree grid, is based on ship and aircraft observations before the satellite era, i.e., before 1981, passive microwave-based estimates obtained from the Goddard Space Flight Center using the NASA team algorithm through 1996, and the NCEP weekly analysis, also based on the NASA team algorithm, thereafter [*Rayner et al.*, 2003]. The ice concentration in the ERA-40 forcing data set, which is used for assimilation in the ice–ocean model, is based on the Hadley data before 1981 and on the weekly NCEP analysis thereafter, so the model representation of the ice concentration and extent is very close to the values in HadSST [*Fiorino*, 2004]. The two data sets differ primarily in that the ERA-40 ice concentration is at a resolution of 2.5 degrees and has been interpolated to daily time steps. The ice extent is computed as the area with ice concentration greater than 0.15. The HadSST data show that sea ice extent in the Arctic is in retreat and the pan-arctic ice extent both in March (time of maximum) and September (time of minimum) show significant downward trends (Figure 1). *Meier et al.* [2007] report a significant discontinuity in the HadSST ice concentration data in 1997, when the NCEP analysis was incorporated. The discontinuity amounts to 8% of the ice extent in September, based on comparisons of an overlap period of 1997–2003. This discontinuity will unfortunately increase the errors of the statistical models and the forecasts, errors which are accounted for in the computed forecast skill scores. Discontinuities in the sea ice data record, such as those identified by *Meier et al*. are included in the error statistics and forecast skills. The removal of such continuities would likely improve results.

2.1.3. Assimilation of Open-Ocean SST

[15] The sea surface temperature in the model is determined by the energy balance of the top layer of the ocean, 10 m thick. If the surface energy fluxes are in error, the temperature of this layer will be incorrect and the error will propagate to deeper levels in the model ocean. Errors in the energy fluxes are corrected by assimilating the observed SST. Observations of sea surface temperature are assimilated in the open water areas only through a nudging procedure with a 15-day time constant. We use the SST data from the ERA-40 and operational ECMWF data sets so that there are no large discrepancies between the adjusted model SST and the forcing air temperatures. This is because the same SSTs are used in the atmospheric model that generates the air temperatures. The ERA-40 SST fields are, like the ice concentration, based on the Hadley Centre monthly mean SST fields before 1981, on the weekly Reynold's SST fields (from NCEP) through 2001, and on daily ECMWF operations fields thereafter [*Fiorino*, 2004]. The fields are based largely on in situ data from ships and buoys before 1981 with the addition of satellite data thereafter.

[16] The assimilation of SST in the open water areas increased the model mean surface temperature by up to 5 K in the Nordic seas in the fall and winter and decreased the surface temperature by up to −5 K in these same areas in summer. The increased winter surface temperatures propagated throughout the Arctic Basin, most notably at depths between 100 and 300 m. Maximum annual mean temperature differences of +3 K were found within the basin at 173 m depth with the assimilation of SST in open water areas.

2.1.4. Assimilation of Ice Concentration

[17] The ice concentration from the ERA-40 and operational analyses, which are based on the Hadley Centre data set, are assimilated in a nudging procedure outlined in *Lindsay and Zhang* [2006]. In this procedure the model estimate of the ice concentration is nudged toward the observations in a manner that gives heavy weighting to the observations when there is a large difference between the two. This essentially assimilates ice extent because if both the model and the observations show similar amounts of ice, the observations are not heavily weighted. The procedure makes the assimilation scheme relatively insensitive to the large observational errors in passive microwave estimates of the ice concentration during the summer.

2.1.5. Climate Indexes

[18] Four different climate indexes are used as possible predictor variables. These include the Arctic Oscillation (AO) index obtained from the National Weather Service Climate Prediction Center (CPC), the North Atlantic Oscillation (NAO, from the CPC), the Pacific North American pattern (PNA, from the CPC), and the Pacific Decadal Oscillation (PDO) obtained from the Climate Impacts group at the University of Washington. In each case a three-month moving average was used in the predictions.

Table 1. Candidate Variables[a]

Name	Definition	CWT
Prst	Persistence of observed total ice extent from earlier months	
AO	Arctic oscillation, 3-month average	
NAO	North Atlantic oscillation, 3-month average	
PDO	Pacific decadal oscillation, 3-month average	
PNA	Pacific North American index, 3-month average	
IX	Ice extent: cells with $I_{conc} > 0.15 = 1$, others = 0	x
IC	Ice concentration	x
H	Mean ice thickness	x
G1	Fractional area of open water and ice less than 0.66 m thick	x
G2	Fractional area of open water and ice less than 1.93 m thick	x
G3	Fractional area of open water and ice less than 4.20 m thick	x
OT005	Ocean temperature centered at 5-m depth (0−10 m)	x
OT045	Ocean temperature at 45-m (40−50 m)	x
OT126	Ocean temperature at 126-m (110−150)	x
OT234	Ocean temperature at 234-m (200−270 m)	x

[a]Those marked in the CWT column indicate model fields that are processed to form correlation weighted time series.

2.2. Statistical Forecast Model

[19] Briefly, the forecast procedure for predicting the ice extent with the statistical forecast model for a particular region and month consists of the following steps.

[20] • Select a set of candidate forecast variables from the hindcast model fields and climate indexes.

[21] • Select a time interval for determining the forecast model (so that it can be tested with forecasts beyond the chosen interval) and choose a lead time for the forecast (the predictor month).

[22] • Convert time-dependent model fields (from the predictor month) to time-dependent scalars in a way that preserves the correlation of the field with the forecast ice extent.

[23] • Determine the linear prediction equation by selecting the two variables that best fit the observations over the interval.

[24] • Determine the error of the forecast expression in predicting the ice extent for one or two years after the fit interval, using independent input data also from after the interval.

2.2.1. Candidate Variables

[25] Selection of candidate variables (Table 1) is a critical element in formulating an empirical forecast model. We include 1) the past history of the observed total ice extent in order to evaluate the importance of persistence; 2) climate index variables to represent the state of the atmospheric circulation over broad scales and because previous research points to the possible utility of these measures; 3) model-based fields representing the state of the ice cover (gridded ice concentration, ice extent, and mean ice thickness) because they are directly related to the total ice extent; 4) model estimates of the cumulative area of ice and open water less than three ice thicknesses (0.66, 1.93, and 4.20 m, the upper bounds of the three thinnest ice thickness classes) because each represents the open water area fraction after the melt of a fixed thickness of ice; and 5) ocean temperature, taken from four non-adjacent model levels. The ocean temperatures from these levels were included because in the top level, 5 m, the water temperature is also the model SST. It is at the freezing point in the presence of ice and is most directly impacted by vertical heat fluxes. At the lowest level considered, 200—270 m (centered at 234 m), vertical heat fluxes are weaker due to reduced mixing and thus horizontal advective processes associated with Atlantic Water transport are more important. The temperature at the two other levels (centered at 45 m and 126 m) are included to determine if intermediate depths are important. Deeper levels were not considered because of their even more limited interaction with the surface.

2.2.2. Model Fields

[26] The reanalysis model fields are an estimate of the variable at each grid cell. To greatly reduce the number of candidate variables considered for the forecast model, we condense each monthly field, which consists of thousands of numbers, to a single number in a manner that conserves the relationship between the field and the forecast variable. This is done by finding a weighted average of each monthly field in which the weighting is the correlation map of the field with the forecast ice extent. The result is the correlation-weighted time series (CWT) of each field [*Drobot et al.*, 2006]. Possible alternatives might be empirical orthogonal functions (EOF) for the weighting maps and the resulting principle components (PC) for the time series. To properly represent the field, several PC would be required and it is possible that none of them individually is well correlated with the forecast variable. The CWT is a weighting method that preserves the correlation in a single time series.

[27] Let $R_{i,j}(m, \lambda)$ be the temporal correlation of the field $F_i(m-\lambda, y)$ at the predictor month (with lead time λ) with the ice extent $I_{\text{ext}}(m, y)$ (at the forecast month m) for each location j over the selected time interval, i.e., for the years y from y_{strt} to y_{end}. The weighted average of the field for year y is then

$$x_i(m-\lambda, y) = \frac{\sum_j F_{i,j}(m-\lambda, y) R_{i,j}(m, \lambda)}{\sum_j R_{i,j}(m, \lambda)}. \quad (1)$$

[28] The summations are only over locations that include just the positive or just the negative correlation areas, whichever has the largest integral. Other areas are given zero weight. In other words, if the field is primarily positive, only the positive areas are included, and if it is primarily negative, only the negative areas are included so that the smaller areas do not reduce the influence of the larger areas. Only the areas in the Arctic Ocean and the peripheral seas, including the Bering, Barents, Greenland, and Norwegian seas are used. The CWT is found for each model field considered and for each pair of forecast and predictor months, m and m-λ.

[29] Four samples of the correlation maps used to create the CWT for the September pan-arctic I_{ext} for different prediction months and variables are shown in Figure 2. For each model field variable and at each lead time a map of the correlation coefficient with the September observed ice extent is computed. This map is then used as a weighting field to determine the mean value of the field for each month. As seen in the figure, the ice concentration correlation field is most heavily weighted near the ice edge, where there is substantial variability, while the G2 (area fraction

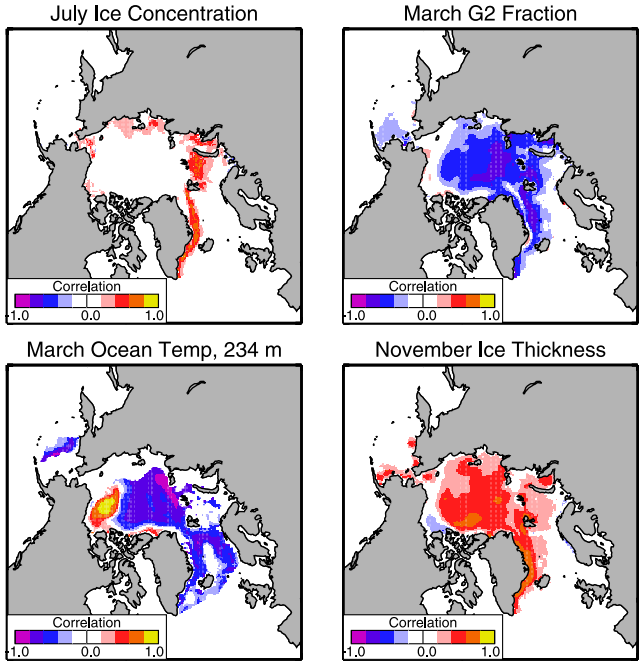

Figure 2. Correlation maps of the pan-arctic September mean ice extent for four different variables at four different lead times. These maps are used to form the correlation-weighted time series (CWT) of each of the variables. G2 is the area fraction of ice and water less than 1.93 m thick (Table 1).

with ice less than 1.93 m thick) and the mean thickness maps are heavily weighted in the interior of the basin and in the Greenland and Norwegian seas. The ocean temperature correlation map shows heavy weighting in a broad region north and south of Fram Strait. The small area with a positive correlation is set to zero weighting. Most of the correlation maps change with the lead time, but because of the small amount of seasonal variability in the deep ocean temperature, the correlation maps for the ocean temperature change very little with the predictor month.

2.2.3. Statistical Model

[30] We use a least squares multiple linear regression model that includes one or more predictor variables from the predictor month to estimate the ice extent for a forecast month [recall $I_{ext}(m, y)$ is the observed ice extent in month m and year y]. A regression model is determined for the years in a fit interval *int:* y_{strt} to y_{end}. The number of years is $N_{yrs} = y_{end} - y_{strt} + 1$. The estimated ice extent based on training data from a given interval is $I_{ext}(m, y|int)$. The predictor variables are $x_i(m-\lambda, y)$, where i indicates the variable and λ is the lead time. The regression equation is then

$$\hat{I}_{ext}(m,y|\text{int}) = a_{0,\text{int}} + \sum_{i=1}^{nterms} a_{i,\text{int}} x_i(m-\lambda,y) + \varepsilon(m,y|\text{int}), \tag{2}$$

where m is the forecast month, $m-\lambda$ is the predictor month (if the predictor month is from the year before that of the forecast month, y is reduced by one for the predictor variables), and ε is the error. The constants $a_{0,int}$ and $a_{i,int}$, are determined with the least squares procedure using the years y_{strt} to y_{end} for the fit.

[31] Variables are selected with a forward stepwise regression procedure. They are added one at a time in the order in which they are able to explain the variance of the residuals from the previous set of predictors, starting with the one most highly correlated with $I_{ext}(m, y)$, until a predetermined number of terms are found or the coefficients are not statistically significant. In these analyses only one variable is usually significant according to the p-value of the coefficient, although a second variable is found to be significant in some cases. The goodness of the model fit within the fit interval is given by the R^2 statistic for the fit,

$$R^2 = 1 - \frac{\sigma_\varepsilon^2}{\sigma_{I(m|\text{int})}^2}, \tag{3}$$

where σ_ε^2 is the variance of the error and $\sigma_{I(m|\text{int})}^2$ is the variance of the observed ice extent for month m. A backwards selection procedure was also tested. This resulted in some changes in the variables selected for some lead times but the forecast skill scores (see below) were never improved. Variance inflation factors show that for the two-parameter models collinearity is not a problem.

2.3. Forecast Error Evaluation

[32] The error of the forecast model is evaluated by making prognostic forecasts using the statistical model, not on evaluating the fit of the model to a sample of withheld data from within the fit interval, as is done in some studies. The distinction is important because the mean state of the ice-ocean system changes and the statistical relationships between the variables cannot be assumed stationary. While the forecast model does assume stationarity, our evaluation of the errors should not. If the system is stationary, the skill of the forecast would be given by the R^2 value of the fit, but if the correlations between the variables are changing over time the forecast skill may be much smaller.

[33] Forecasts are found by using CWT weighting maps and the coefficients from each fit interval to estimate the ice extent in the subsequent two years. For example, one might formulate the forecast model (determine CWT, select variables, and determine coefficients) using years 1–35, then use that model to forecast the ice extent in years 36 and 37 using predictor data from the same two years. The procedure can be repeated for different fit intervals, which may be overlapping, and the error in the forecasts can be found for each interval.

[34] Recall the model fit period is *int:* y_{start} to y_{end}. The CWT variables for the subsequent years $y_{end} + 1$ and $y_{end} + 2$ are determined from (1) using the field variables from those two years and the correlation fields found for the fit interval. The forecast ice extent is

$$\hat{I}_{ext}(m,y|\text{int}) = a_{0,\text{int}} + \sum_{i=1}^{nterms} a_{i,\text{int}} x_i(m-\lambda,y) \tag{4}$$

where y is $y_{end}+1$ or $y_{end} + 2$. The coefficients $a_{i,int}$ refer to coefficients determined for the interval y_{start} to y_{end}. Intervals of 35 years are used for each fit and the fit intervals shift forward starting at years 1, 2, . . .,13. For each fit interval the ice extent for the subsequent two years is estimated. A total of $N_f = 25$ forecasts can then be made.

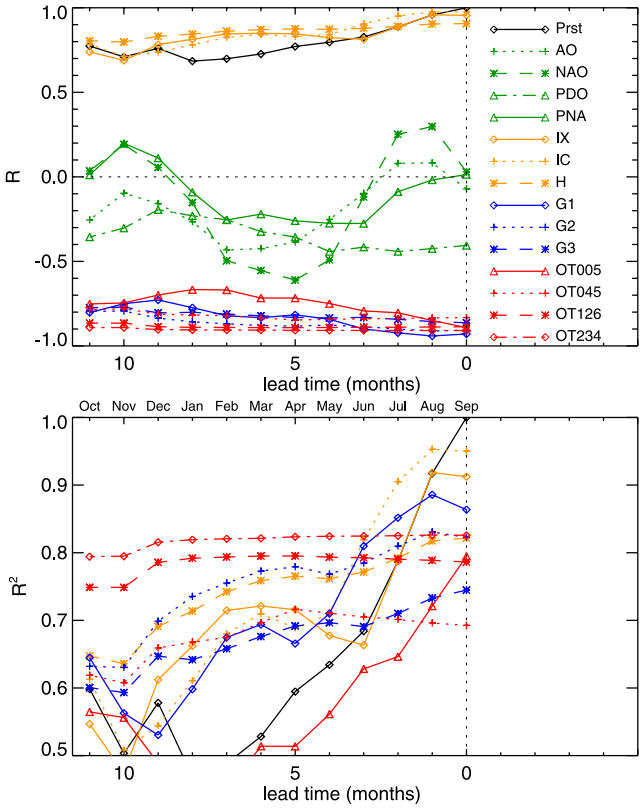

Figure 3. Lagged correlations of each candidate variable with the basin-wide September mean ice extent: (a) Correlations, (b) Squared correlations (see Table 1 for definitions). Note that the climate indexes in the upper plot are off the bottom in the lower plot.

More than two test years is not warranted because the errors in the forecasts increase as the time of application of the forecast model is farther removed from the fit interval, evidence of nonstationarity in the system. Shorter fit intervals would allow for more test samples but the forecast skill is found to decrease with shorter fitting intervals. The forecast error variance for the N_f forecasts is then

$$\sigma^2_{ferr} = \frac{1}{N_f} \sum_{k=1}^{N_f} \left[I_{ext}(m, y|\text{int}_k) - \hat{I}_{ext}(m, y|\text{int}_k) \right]^2. \quad (5)$$

[35] This procedure uses the most recent 35 years to determine the coefficients needed to forecast the next two. Note that these error estimates are far from independent because the intervals almost entirely overlap and two tests are made for each fit interval. However, the errors here are determined from actual forecasts and can better reflect the influence of the nonstationary aspects of the data sets than statistics computed by randomly withholding some small fraction of the data.

[36] The forecast skill is determined relative to a reference value, in our case either the variance of the observed ice extent about the climatological mean or about the previous year's extent. These two measures represent alternative simple methods of predicting the ice extent and the use of a forecast model is only justified if the error is less than that of the simple alternatives. The skill is

$$S = 1 - \frac{\sigma^2_{ferr}}{\sigma^2_{ref}}. \quad (6)$$

[37] For the skill relative to climatology σ^2_{ref} is the variance of $I_{ext}(m, y)$ (about its mean) and for the skill relative to the previous year it is the mean-sum-of-squares of $I_{ext}(m, y) - I_{ext}(m, y-1)$. The error variance is larger for climatology, so the forecast skill score relative to climatology, S_{Clim}, is greater than that relative to the previous year, S_{PrevYr}. A perfect forecast would have a skill of 1.0 and any forecast with a skill less than zero is worse than simply using the reference value. A skill somewhat greater than zero is needed to justify the effort of using the forecast method, but how much greater depends on the specific application. Note that the skill of the fit within the interval, relative to climatology, is R^2, but this is not a forecast skill.

3. Pan-Arctic September Ice Extent

3.1. Lagged Correlations

[38] To begin, the lagged correlation with the observed September ice extent is determined for each of the candidate variables in Table 1 (Figure 3). The squared correlation is also shown so that variables with both positive and negative correlations can be compared directly and so that the fraction of the variance explained in a one-variable model can be seen. The figure shows that the climate indexes (green) all have a significant correlation at some lead times but in no month do they have a better correlation than persistence of the ice extent. They are all off the bottom of the R^2 plot, less than 0.5. The low correlations of the climate indexes compared to the ice and ocean variables reflects the fact that the model ice and ocean system incorporates all impacts of the changing circulation patterns while the indexes measure limited aspects of the hemispheric climate.

[39] The model variables have high correlations in part because of the construction of the CWT values in which the fields are spatially weighted by the correlations with the ice extent, thereby maximizing the correlation. Among the model ice variables (orange), the ice extent is most correlated with the ice concentration for short lead times, with a positive correlation as expected. The area of open water and ice less than 0.66 m thick (G1), or 1.93 m thick (G2), is as well or better correlated for longer lead times, with a negative correlation because more thin ice and open water in the early summer leads to lesser ice extent in September. At one year (October) the mean ice thickness is as well correlated with the September ice extent as G1 and G2. In fact throughout the year there are several model variables that are nearly equivalent in their degree of correlation with the September ice extent.

[40] The CWT ocean temperatures (red) are well correlated with the ice extent at all lead times with generally higher correlations at deeper depths. This is because the ocean temperatures at these levels have little year-to-year variability and because the CWT procedure has determined a spatial weighting that maximizes the correlation between the ocean temperature and the ice extent. The ocean temper-

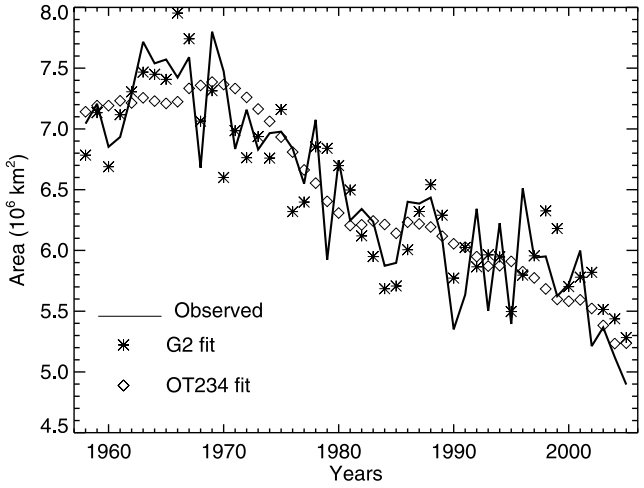

Figure 4. The observed September mean ice extent and the model fit for a six-month lead time (March) using just the G2 variable (area fraction with less than 1.92 m ice) or using just the ocean temperature at 234 m. The R^2 value for the G2 fit is 0.77 and for OT234 fit is 0.81.

atures are negatively correlated with the ice extent, which is consistent with warm water temperatures reducing the ice extent. The difference in the amount of variability of one of the ice parameters and of the ocean temperature are reflected in how a one-parameter model reproduces the observed ice extent. Figure 4 shows the observed September ice extent and the one-parameter model fits for the G2 ice fraction and the OT234 ocean temperature at six months lead. The OT234 fit has a higher R^2 value, 0.81 versus 0.77, because it has less high-frequency uncorrelated variability than the G2 parameter.

[41] The ocean temperature better captures the decadal-scale variability in the ice extent than those variables describing the state of the ice cover, which have large year-to-year variability that is not well correlated with the observed September ice extent for lead times of six months or more.

3.2. Forecasts of September Ice Extent

[42] To forecast the observed September ice extent, the forecast model is fit for two terms with lead times of 0 to 11 months (Table 2). The trivial predictor persistence is not included for lead zero, when the ice concentration is best correlated with the current ice extent. Otherwise the first term selected follows what is expected from Figure 3; the first two lead times have the ice concentration as the primary variable, then the ocean temperature at 234 m is selected for the rest of the lead times. The coefficient of the first term is always highly significant (p-value very near zero) while that of the second is often not significant (p-value greater than 0.05). The second variable selected for lead times of six months or more is either the NAO or the AO, but the R^2 value of the fits is increased by only a few percent in each case. The R^2 value of the fit is above 0.95 at zero lead and decreases monotonically but is above 0.80 for all lead times, substantially higher than the values reported by *Drobot et al.* [2006] using just satellite-based information. This confirms the hypothesis that the ice–ocean model simulations provide additional information that can aid in the prediction of ice extent. The high values of R^2 indicate that the CWT procedure is able to extract good correlations of the model fields with the forecast ice extent and that the model state, both in ice parameters as well as in ocean parameters, provides excellent indicators of the future state of the ice pack. Because there is little month-to-month variability in the deep ocean temperature, the R^2 values remain nearly constant for lead times of five months to one year.

[43] One measure of the system's nonstationary nature is seen in a consistent bias in the forecasts. The bias values for these forecasts are positive for all lead times and show that the forecast extents are too high, indicating there is typically less ice and more open water than the forecast model predicts. The ice extent appears to be declining faster than historical relationships indicate. The bias values in Table 2 are squared and normalized by the variance of I_{ext} so that they may be compared to the climate-relative skill scores. For example, in June the climate-relative skill is reduced by 0.159 in the two-parameter model because of the bias.

[44] The two right columns of Table 2 refer to the forecast skill based on 25 (non-independent) forecasts, all made in the last 13 years of the record. The R^2 values and skill scores for two-variable models at different lead times are shown graphically in Figure 5. The climate-relative skill of the predictions is lower than the R^2 values of the model fit.

Table 2. Variables and Fit Parameters for the Pan-Arctic Observed September Mean Ice Extent for One- and Two-Variable Forecast Models[a]

Lead Time	Month	Variable	Coeff.	p-value[b]	R^2	Bias[2c]	S_{Clim}	S_{PrevYr}
0	Sep	IC PDO	9.791 −0.064	0.000 0.081	0.950 0.956	0.000 0.002	0.968 0.964	0.930 0.922
1	Aug	IC NAO	9.858 0.042	0.000 0.589	0.953 0.954	0.007 0.005	0.954 0.959	0.900 0.911
2	Jul	IC NAO	11.685 0.132	0.000 0.095	0.905 0.914	0.070 0.048	0.800 0.801	0.561 0.562
3	Jun	OT234 G1	−0.620 −5.663	0.000 **0.001**	0.825 0.872	0.219 0.159	0.580 0.634	0.077 0.197
4	May	OT234 G2	−0.725 −5.813	0.000 **0.018**	0.824 0.853	0.029 0.015	0.762 0.763	0.476 0.479
5	Apr	OT234 PDO	−1.178 0.107	0.000 0.173	0.824 0.837	0.029 0.017	0.759 0.760	0.471 0.472
6	Mar	OT234 AO	−1.045 −0.116	0.000 0.222	0.821 0.833	0.028 0.017	0.755 0.773	0.463 0.502
7	Feb	OT234 AO	−1.029 −0.167	0.000 **0.042**	0.821 0.844	0.029 0.066	0.756 0.787	0.465 0.533
8	Jan	OT234 AO	−1.064 −0.188	0.000 **0.024**	0.819 0.847	0.030 0.076	0.756 0.764	0.464 0.481
9	Dec	OT234 AO	−1.083 −0.154	0.000 0.088	0.816 0.835	0.031 0.049	0.755 0.759	0.461 0.470
10	Nov	OT234 AO	−1.075 −0.162	0.000 0.106	0.814 0.832	0.031 0.051	0.754 0.729	0.460 0.404
11	Oct	OT234 NAO	−1.095 −0.217	0.000 **0.022**	0.812 0.842	0.032 0.053	0.753 0.748	0.458 0.446

[a]The coefficients, p-values, and multiple R^2 values are for the fit with all years. The skill values are based on forecasts.
[b]p-values for the second parameter less than 0.05 are in bold.
[c]Bias is normalized by the variance of the September ice extent. The bias is always positive for these forecasts.

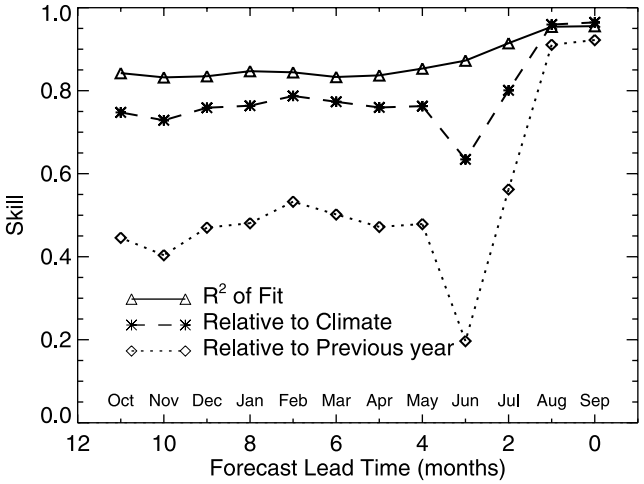

Figure 5. Forecast skill scores for the pan-arctic forecast of the September mean ice extent for different lead times. The line marked Fit is the R^2 value of the two-parameter model fit over the entire time interval. The other lines are the forecast skill scores relative to climatology or to the previous year.

If the correlations between the dependent and independent variables were stationary, these skill scores would be quite similar to the R^2 values. The climate-relative forecast skill scores of the two-parameter models are all above 0.63. Interestingly, they increase at long lead times even though the R^2 values do not, suggesting that the fall ocean temperature information may be a better predictor of the summer ice extent than the spring ocean temperature. For most lead times the skill scores are not improved with two-parameter models compared to one-parameter models even though the R^2 values are slightly better.

[45] Much of the skill relative to climatology is due to the large trend in the ice extent. The trend accounts for 76% of the variance in the September I_{ext}, very near the R^2 values of many of the model fits. The large trend in the ice extent means that the previous year is often a better predictor of the current year than the climatological value, hence when the forecast skill is computed relative to the previous year, S_{PrevYr}, it is much lower than with respect to climatology, S_{Clim} (Table 2 and Figure 5).

4. Seasonal and Regional Variability in Forecast Skill

[46] How does the predictive skill change with the forecast month? During winter the variability and the trend in the pan-arctic ice extent is much less than during the summer (Figure 1) so the skill of the predictions also should change substantially. The fitting and skill evaluation procedures are applied to make six-month forecasts and error evaluations for each month of the year (Table 3 and Figure 6).

[47] The R^2 values of the model fit over the entire 48-year period are consistently high, above 0.68 for all months. The climate-relative forecast skill, however, has a strong seasonal cycle, with the worst skill in predicting the ice extent for the late winter and early fall. The months of June and December have high skill values, greater than 0.85 relative to climatology. In all months the best predictor variable is the ocean temperature at 5 m, 126 m, or 234 m. Again, the skill values relative to the previous year are much lower than relative to climatology, and indeed there is no skill in predicting April or October ice extents.

[48] These procedures are easily adapted to forecast the ice extent in regions smaller than the entire basin. With smaller regions the skill scores are substantially smaller, and forecasts for just three months are made here. The three-month (from June) predictions of the regional September ice extent for six 45° longitudinal sectors show that the R^2 values and the climatological forecast skill scores for each of the sectors (Table 4 and Figure 7) are best in sectors corresponding to the Greenland, Barents, and Kara seas. However, the forecast skill scores are positive, i.e., better than climatology, for all sectors in the Northern Sea Route (sectors 1–4). The only sector with significant interannual variability but with no skill is that of the Beaufort Sea, with an R^2 value over the entire interval of only 0.43. Much of the negative skill score is due to the large bias in the predictions for this sector caused by rapidly changing relationships between the predictor variables and the regional ice extent. The correlation maps of the primary predictors selected for four sectors (Figure 8) show maxima near each of the sectors, but there are some significant correlations well outside the sectors, showing not only that

Table 3. Seasonal Six-Month Predictions of the Pan-Arctic Ice Extent for One-and Two-Term Forecast Models[a]

Predictor Month	Forecast Month	Variable	Coeff.	p-value	R^2	Bias^2	S_{Clim}	S_{PrevYr}
Jul	Jan	OT126 G3	−0.275 −3.777	0.000 0.112	0.699 0.727	0.155 0.046	0.501 0.634	0.000 0.267
Aug	Feb	OT005 PNA	−0.401 0.062	0.000 0.491	0.688 0.697	0.089 0.069	0.474 0.479	0.126 0.135
Sep	Mar	OT005 OT234	−0.314 −0.204	0.000 0.124	0.781 0.801	0.137 0.114	0.539 0.556	0.011 0.049
Oct	Apr	OT126 AO	−0.588 −0.134	0.000 0.085	0.795 0.816	0.040 0.048	0.575 0.591	−0.085 −0.043
Nov	May	OT126 AO	−0.835 −0.082	0.000 0.441	0.864 0.869	0.001 0.003	0.824 0.835	0.309 0.353
Dec	Jun	OT126 NAO	−0.810 −0.097	0.000 0.207	0.881 0.889	0.002 0.010	0.891 0.898	0.529 0.558
Jan	Jul	OT126 G1	−0.813 −2.829	0.000 **0.026**	0.881 0.899	0.007 0.011	0.844 0.848	0.473 0.488
Feb	Aug	OT126 AO	−1.063 −0.177	0.000 **0.030**	0.877 0.895	0.016 0.033	0.780 0.817	0.260 0.384
Mar	Sep	OT234 AO	−1.045 −0.116	0.000 0.222	0.821 0.833	0.028 0.017	0.755 0.773	0.463 0.502
Apr	Oct	OT234 G1	−0.721 −2.712	0.000 0.175	0.802 0.817	0.283 0.226	0.422 0.486	−0.434 −0.276
May	Nov	OT126 OT005	−0.461 −0.564	0.000 **0.045**	0.772 0.801	0.001 0.000	0.808 0.756	0.523 0.393
Jun	Dec	OT126 G3	−0.389 −4.619	0.000 **0.037**	0.811 0.837	0.030 0.008	0.792 0.853	0.304 0.508

[a]See Table 2.

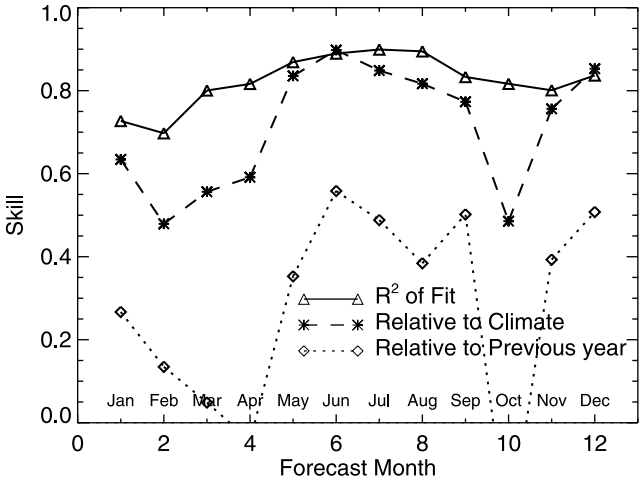

Figure 6. Skill scores for six-month forecasts of the pan-arctic mean ice extent for each month of the year, with lines as in Figure 5.

ice may advect into the region, but that there is also significant covariability in the ice properties over large areas.

[49] *Drobot* [2007] presents a similar technique to make predictions for regional sectors, albeit for somewhat differently defined regions and for the minimum ice extent rather than for the September mean. The skill scores are computed by withholding data from within the fit interval (23 years) rather than by making predictions. They use the CWT procedure with five satellite-based candidate predictors: ice concentration, multiyear ice concentration, surface temperature, and surface albedo. The R^2 values of the fits are similar in Kara Sea [0.73 versus 0.63 in the present study, but are higher in the Beaufort Sea (0.80 versus 0.41) and in the Laptev Sea (0.72 versus 0.56)]. The better fits may be because they use a shorter time interval for the fits so the recent trends are more apparent.

[50] One reason that the skill scores presented here are smaller for the sectors than for the entire basin is that the fraction of the variability accounted for by the trends is smaller. The R^2 values of the fit of a trend line for the September ice extent in the individual sectors over the period 1958–2005 are 0.18–0.56 compared to 0.76 for the entire basin.

5. Discussion

[51] The forecast procedures presented here show considerable skill, when compared to historical variability, in predicting the observed September pan-arctic ice extent up to one year in advance using model simulation results for the predictors. The predictor responsible for much of the skill for short lead times (one or two months) is the ice concentration, but for longer lead times the best predictor is the ocean temperature at a depth of 234 m. It is understandable that low ice concentrations in the early summer leads to low ice extent in the late summer, but at longer lead times the ocean temperature is the best predictor. Why? First, the relatively sluggish ocean operates on intrinsically longer timescales than the overlying sea ice pack [e.g., *Morison et al.*, 2006; also Figure 4]. Second, although upward heat flux from several hundred meters depth to the surface is suppressed by a strong halocline in much of the central Arctic Ocean [e.g., *Steele and Boyd*, 1998], this heat flux can be quite strong in the North Atlantic sector, i.e., the Nordic Seas and the Nansen Basin of the Arctic Ocean [e.g., *Steele and Morison*, 1993]. These latter areas lack a strong permanent halocline [*Rudels et al.*, 1996]. Thus northward heat transport from the North Atlantic Ocean can be correlated with the sea ice cover [*Zhang et al.*, 2004].

[52] The CWT procedure is designed to determine a spatial weighting pattern that maximizes the correlation with the observed September ice extent, and because of the strong trend in the extent the best correlation is found in a broad region of the Arctic Ocean deep water temperature that shows a similar pattern of low-frequency variability. Both the ice and the ocean, in particular regions, are responding to a general warming of the Arctic region. The ice variables, such as concentration or thickness, show significant year-to-year variability in addition to the trend that is not well correlated to the ice extent at the longer lead times.

[53] The importance of the trend is seen by comparing the lagged correlations of the predictor variables with the pan-arctic ice extent, but with the trends removed from both the ice extent and the predictor variables (Figure 9). These

Table 4. Regional Three-Month Predictions of the Ice Extent[a]

Sector	Longitude	Variable	R^2	Bias[2]	S_{Clim}	S_{PrevYr}
1, Barents Sea	15–60	G2	0.724	0.02(−)	0.77	0.713
2, Kara Sea	60–105	G1	0.633	0.00	0.74	0.794
3, Laptev Sea	105–150	G1	0.586	0.01	0.18	0.578
4, East Siberian Sea	150–195	G1	0.668	0.15	0.08	−0.166
5, Beaufort Sea	195–240	OT234	0.410	0.76	−0.67	−0.329
8, Fram Strait	330–015	IC	0.680	0.00	0.54	0.326

[a]See Table 2. All of the p-values for the first term are less than 0.01, so they are not shown, and for the second term are greater than 0.05.

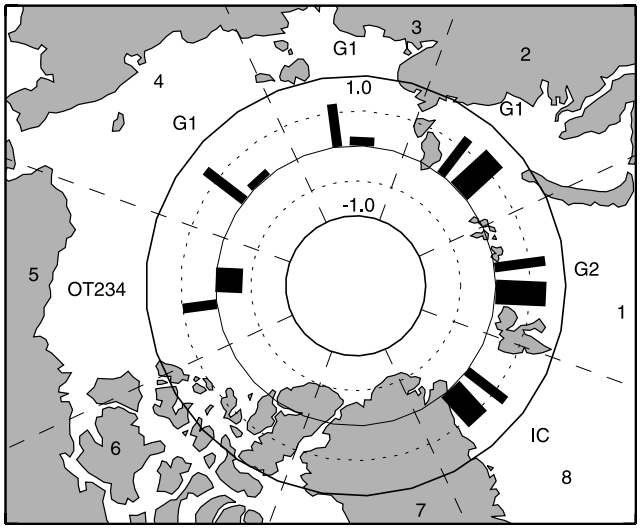

Figure 7. Map of R^2 values of the model fit (thin bars) and the climate-relative skill scores (thick bars) of three-month predictions for the observed September ice extent in individual sectors. The primary predictive variable is shown for each sector. There is no variability in the ice extent in sectors 6 and 7.

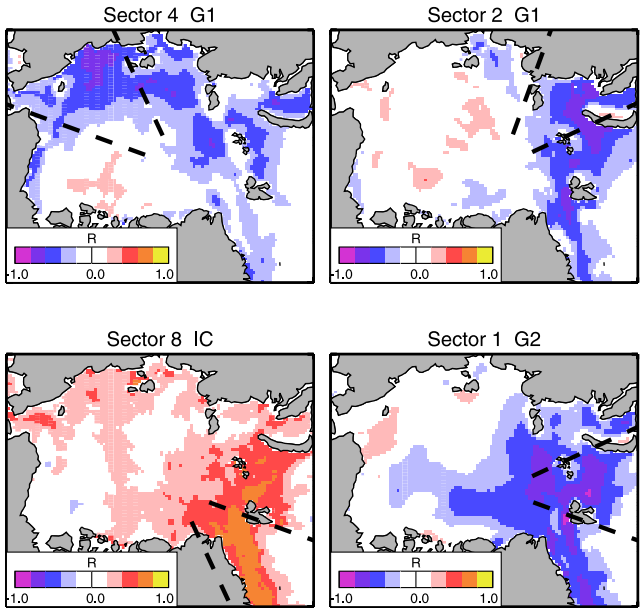

Figure 8. Correlation maps of the primary three-month predictive variables for four different sectors. The correlations are with the observed sector-mean September ice extent.

detrended lagged correlations are much lower than those plotted in Figure 3 and the ordering of the most highly correlated variables differs. The ice variables (extent, concentration, thickness, and area fractions) are generally more highly correlated with the ice extent than the ocean temperatures. Also, with lead times of greater than three months, all of the R^2 values are less than 0.5. Consequently, the forecast skill scores for these lead times are negative for detrended data. Except for the trend, much of the predictive information in the ice-ocean system is lost for lead times greater than about three months.

[54] The predictability of the pan-Arctic ice extent has a strong seasonal dependence, with the best six-month predictions made for the summer (May–September) or the early winter (November–January). In the late winter the variance of the ice extent is less than in other seasons and a smaller fraction of it is predictable.

[55] The three-month forecast skill for regional ice extents is generally smaller and there is no skill in some sectors because of limited variability in the September ice extent. The skill is highest in the Fram Strait sector because of the high correlation between the September ice extent and the mid-thickness ice fraction, primarily in the region near the North Pole and in the eastern part of the basin. There is positive skill in all sectors of the Northern Sea Route, north of Europe and Siberia. These predictions could easily be implemented in an operational forecast environment to support planning of shipping activities.

[56] The optimal predictors determined here are not necessarily directly related to any specific observations that may be made at specific locations. The method does not suggest where or what kind of observations would improve the forecasts, as the predictors are dependent on the entire model fields. Any observations that improve the model representation of the state of the ice-ocean system, either through creating better physical representations or better forcing fields or through assimilation, might improve the forecasts. However, this study may indicate the limits of predictability of ice conditions with a linear empirical approach. An improved ice-ocean model would not necessarily improve the forecasts.

[57] The high skill scores obtained for the pan-arctic ice extent predictions using the ERA-40 data can be attributed to three main causes: 1) the region is relatively large and easier to predict than smaller regions because the variability is reduced through averaging; 2) the Arctic ice-ocean system has a significant amount of memory; and 3) there is a strong trend in the basin wide ice extent. The additional information provided by a coupled ice-ocean model over surface observations alone does improve the predictability of the ice extent for forecast periods of up to one year.

6. Postscript

[58] The summer melt observed in 2007 is highly remarkable. The August 2007 satellite observations of ice extent have shattered previous records for low ice extent as shown in the National Snow and Ice Data Center Sea Ice Index (nsidc.org/data/seaice_index). How well did our forecasts methods perform? To make real-time forecasts, the National Center for Environmental Prediction (NCEP) reanalysis data, which are available in near real time, were used for forcing the model. The forecast skill scores are

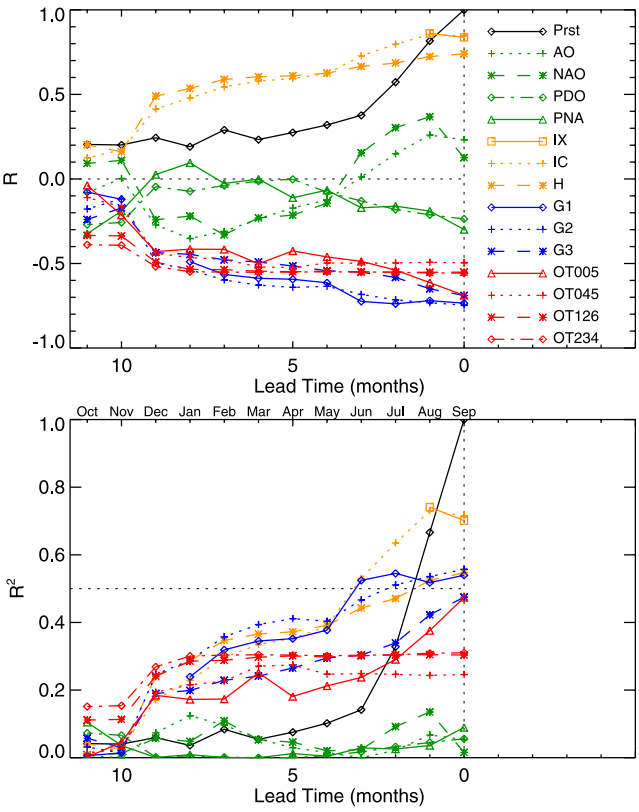

Figure 9. Lagged correlations of the detrended variables with the September pan-arctic ice extent. Both the ice extent and the individual predictors are detrended. The detrending is done before determining the CWT variables.

similar to those obtained using the ERA-40 forcing, although slightly worse. The six-month forecast of the pan-arctic ice extent using March data for August was for very low ice extents but a record low was not predicted to be likely. In other words, the six-month forecast was not accurate. Why? First, the primary predictor in March is the model ocean temperature at 234 m depth, which may not be a good predictor of extreme events; it was selected primarily because it best mirrors the general trend in the pan-arctic ice extent. The poor forecast is due in part because the melt in 2007 was much more extreme than the trend would predict. This would suggest that to better predict year-to-year variability the deep ocean temperature should be avoided. However, predictions using other variables such as the ice thickness or ice concentration did not do substantially better. A forecast made with July ice concentration data does call for a record minimum ice extent in September, though still well above the observed August ice extent. A forecast method based on past correlations can be expected perform poorly when the interrelationships between the variables in the system are rapidly changing and when extreme events occur.

[59] **Acknowledgments.** The ice concentration data were obtained from the British Atmospheric Data Centre, the ERA-40 and ECMWF Operational data from the National Center for Atmospheric Research, the climate indexes from the Climate Prediction Center and the University of Washington Climate Impacts Group. This work was supported by the National Aeronautic and Space Administration Cryospheric Sciences Program under grant NNG06GA84G and NNG04GH52G and by the National Science Foundation Office of Polar Programs under grants ARC-0629326 and ARC-0629312.

References

Barnett, D. G. (1980), A long-range ice forecast method for the north coast of Alaska, in *Sea Ice Processes and Models*, R. S. Pritchard, ed., Univ. Wash. Press, Seattle, 360–372.

Bryan, K. (1969), A numerical method for the study of the circulation of the world oceans, *J. Comput. Phys.*, *4*, 347–376.

Chen, D., and X. Yuan (2004), A Markov model for seasonal forecast of Antarctic sea ice, *J. Clim.*, *17*, 3156–3168.

Cox, M. D. (1984), *A primitive equation, three-dimensional model of the oceans*, GFDL Ocean Group Tech. Rep. No. 1, Geophys. Fluid Dynamics Lab./NOAA, Princeton University, Princeton, N. J.

Drobot, S. D., and J. A. Maslanik (2002), A practical method for long-range forecasting of ice severity in the Beaufort Sea, *Geophys. Res. Lett.*, *29*(8), 1213, doi:10.1029/2001GL014173.

Drobot, S. D. (2007), Using remote sensing data to develop seasonal outlooks for Arctic regional sea-ice minimum extent, *Remote Sens. Environ.*, *111*, 136–147, doi:10.1016/j.rse.2007.03.024.

Drobot, S. D., J. A. Maslanik, and C. F. Fowler (2006), A long-range forecast of Arctic summer sea-ice minimum extent, *Geophys. Res. Lett.*, *33*, L10501, doi:10.1029/2006GL026216.

Dukowicz, J. K., and R. D. Smith (1994), Implicit free-surface method for the Bryan–Cox–Semtner ocean model, *J. Geophys. Res.*, *99*(C4), 7991–8014.

Fiorino, M. (2004), *A multi-decadal daily sea surface temperature and sea ice concentration data set for the ERA-40 reanalysis*, ERA-40 Project Report Series No. 12, 16 pp.

Hibler, W. D., III (1980), Modeling a variable thickness sea ice cover, *Mon. Weather Rev.*, *1*, 943–973.

Holland, D. M. (2000), *Merged IBCAO/ETOPO5 Global Topographic Data Product*, National Geophysical Data Center (NGDC), Boulder CO, digital media.

Johnson, C. M., P. Lemke, and T. P. Barnett (1985), Linear prediction of sea ice anomalies, *J. Geophys. Res.*, *90*, 5665–5675.

Lindsay, R. W., and J. Zhang (2005), The thinning of arctic sea ice, 1988–2003: Have we passed a tipping point?, *J. Clim.*, *18*, 4879–4894.

Lindsay, R. W., and J. Zhang (2006), Assimilation of ice concentration in an ice-ocean model, *J. Atmos. Oceanic Technol.*, *23*, 742–749.

Liu, J., J. A. Curry, W. B. Rossow, J. R. Key, and X. Wang (2005), Comparison of surface radiative flux data sets over the Arctic Ocean, *J. Geophys. Res.*, *110*,C02015, doi:10.1029/2004JC002381.

Meier, W. N., J. Stroeve, and F. Fetterer (2007), Whither Arctic sea ice?: A clear signal of decline regional, seasonally, and extending beyond the satellite record, *Ann. Glaciol.*, *46*, 428–434.

Morison, J., M. Steele, T. Kikuchi, K. Falkner, and W. Smethie (2006), Relaxation of central Arctic Ocean hydrography to pre-1990s climatology, *Geophys. Res. Lett.*, *33*, L17604, doi:10.1029/2006GL026826.

Rayner, N. A., D. E. Parker, E. B. Horton, C. K. Folland, L. V. Alexander, D. P. Rowell, E. C. Kent, and A. Kaplan (2003), Global analyses of sea surface temperature, sea ice, and night marine air temperature, sea ice, and night marine air temperature since the late nineteenth century, *J. Geophys. Res.*, *108*(D14), 4407, doi:10.1029/2002JD002670.

Rigor, I. G., J. M. Wallace, and R. L. Colony (2002), Response of sea ice to the Arctic Oscillation, *J. Clim.*, *15*, 2648–2668.

Rudels, B., L. G. Anderson, and E. P. Jones (1996), Formation and evolution of the surface mixed layer and halocline of the Arctic Ocean, *J. Geophys. Res.*, *101*(C4), 8807–8821.

Schweiger, A. J. (2004), Changes in seasonal cloud cover over the Arctic seas from satellite and surface observations (PDF), *Geophys. Res. Lett.*, *31*, L12207, doi:10.1029/2004GL020067.

Semtner, A. J., Jr. (1976), A model for the thermodynamic growth of sea ice in numerical investigations of climate, *J. Phys. Oceanogr.*, *6*, 379–389.

Smith, R. D., J. K. Dukowicz, and R. C. Malone (1992), Parallel ocean general circulation modeling, *Physica D*, *60*, 38–61.

Steele, M., and T. Boyd (1998), Retreat of the cold halocline layer in the Arctic Ocean, *J. Geophys. Res.*, *103*, 10,419–10,435.

Steele, M., and J. Morison (1993), Hydrography and vertical fluxes of heat and salt northeast of Svalbard in autumn, *J. Geophys. Res.*, *98*, 10,013–10,024.

Walsh, J. E. (1980), Empirical orthogonal functions and the statistical predictability of sea ice extent, in *Sea Ice Processes and Models*, R. S. Pritchard, ed., Univ. Wash. Press, Seattle, 373–384.

Zhang, J. (2005), Warming of the arctic ice-ocean system is faster than the global average since the 1960s, *Geophys. Res. Lett.*, *32*, L19602, doi:10.1029/2005GL024216.

Zhang, J., and W. D. Hibler (1997), On an efficient numerical method for modeling sea ice dynamics, *J. Geophys. Res.*, *102*, 8691–8702.

Zhang, J., and D. A. Rothrock (2001), A thickness and enthalpy distribution sea-ice model, *J. Phys. Oceanogr.*, *31*, 2986–3001.

Zhang, J., and D. A. Rothrock (2003), Modeling global sea ice with a thickness and enthalpy distribution model in generalized curvilinear coordinates, *Mon. Weather Rev.*, *131*(5), 681–697.

Zhang, J., and D. A. Rothrock (2005), The effect of sea-ice rheology in numerical investigations of climate, *J. Geophys. Res.*, *110*, C08014, doi:10.1029/2004JC002599.

Zhang, J., M. Steele, D. A. Rothrock, and R. Lindsay (2004), Increasing exchanges at Greenland–Scotland ridge and their links with the North Atlantic Oscillation and arctic sea ice, *Geophys. Res. Lett.*, *31*, L09307, doi:10.1029/2003GL019304.

R. W. Lindsay, A. J. Schweiger, M. A. Steele, and J. Zhang, Polar Science Center, Applied Physics Laboratory, University of Washington, Seattle, WA 98105-6698, USA. (lindsay@apl.washington.edu)